GROUND TRUTH APPLICATIONS TO ORBIT REFINEMENTS

Robert L. White

The Charles Stark Draper Laboratory

Cambridge, Massachusetts

During the past few years, the C. S. Draper Laboratory has been performing various studies for Goddard Space Flight Center pertaining to the determination and use of spacecraft attitude and orbital ephemeris data to improve the mapping accuracy of an earth-observing multispectral scanner. These studies were conducted for an Earth Observation Satellite (EOS) that is assumed to be in a circular, sun-synchronous orbit with an altitude of 1000 km.

At present, an investigation is being made into the use of known ground targets (that is, landmarks) in the earth sensor imagery, and also stars in combination with known ground targets, to estimate the spacecraft attitude, orbital ephemeris, and the bias drifts of three strapdown gyros. The present study is a covariance analysis where both the Kalman filter and Fraser two-filter smoother are used to process star and landmark measurements to obtain a statistical indication of performance. Star measurements are used to update attitude and gyro bias drift (that is, 6 parameters), and landmark measurements are used to update all 12 state parameters. This study is, for the time, restricted to the use of landmarks in the continental United States, Alaska, and Hawaii, since the primary interest in spacecraft attitude and orbital ephemeris is assumed to be during the observation passes over these regions.

The geometry of a typical pass over the United States is shown in figure 1. The spacecraft maintains a local vertical orientation as shown in the figure, where the body axis, Z_B, is always directed toward the subsatellite point. The star tracker is assumed to be a body-fixed instrument whose optical axis is directed toward zenith. As the spacecraft circles the earth, the stars pass through the 8° square field-of-view (FOV) and are electronically tracked. For the purposes of this study, these stars are artificially generated with random positions in the FOV at the times of measurement. These measurements are uniformly distributed throughout the orbit and only one measurement is made on each star as it passes through the FOV.

On board the spacecraft, there is assumed to be a multispectral scanner whose beam is directed downward and sweeps back and forth across the ground track to generate a swath of imagery 145 km (90 miles) wide (see figure 1). In the present study, a landmark measurement represents the line-of-sight (LOS) of the scan beam at the time of landmark observation. This LOS is completely defined in body coordinates by the scan beam angle for which a random value (within ±4.8°) is selected for each landmark measurement.

Figure 1. Geometry of typical observation pass.

Table 1 defines the five different landmark observation cases used in this study. The case numbers denote the number of orbital passes made over the regions of interest. A pictorial representation of case 4 is shown in figure 2, where the plus signs (+) indicate the nominal locations of the landmarks used for update purposes.

The nominal conditions used to generate most of the performance results are listed below:

- Orbit — Sun-synchronous circular orbit with an altitude of 1000 km

- Gravity model — Central force field

- Spacecraft attitude history — Local vertical with rotation only in pitch

- Star measurements — Error: 5 s (1σ)/axis; number: 20 per orbit (evenly distributed)

- Landmark measurements — Position error: 15 m (1σ) in downrange and crosstrack; number: two/pass

- Gyro error — Random drift rate (1σ) = 0.01°/hr (white noise; quantization (1σ) = 0.1 s

It can be seen that relatively simple models were adopted for the spacecraft attitude history and the gravitational model, since it was felt that these would be sufficient for the purposes of this investigation. Previous studies of attitude determination have shown that the performance results for a nominal attitude history are in fairly close agreement with those for an
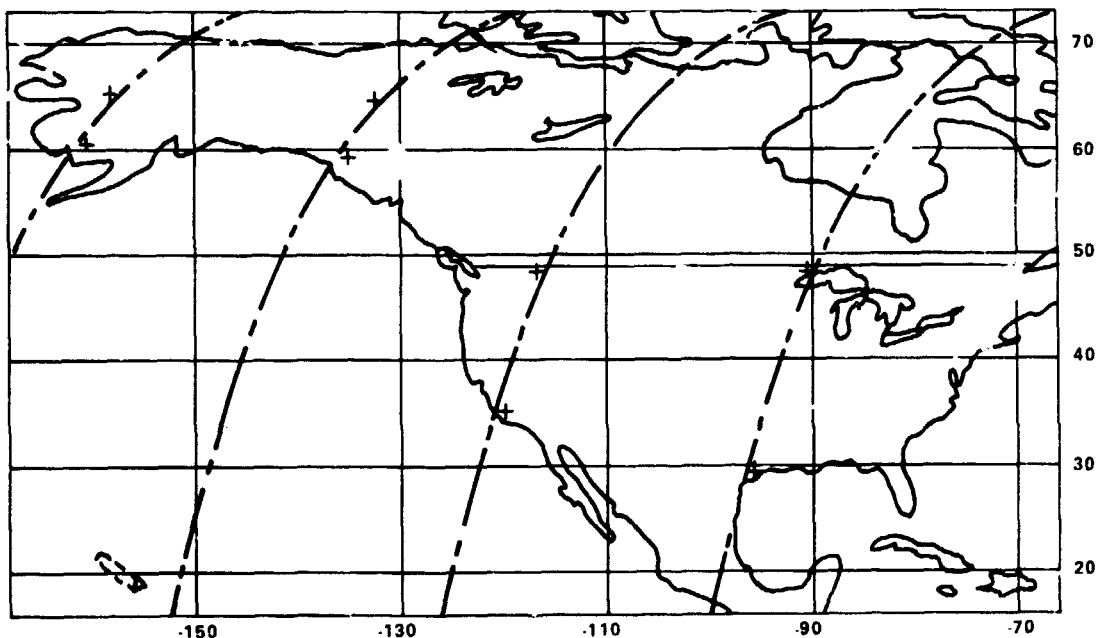

Figure 2. Landmark observation case 4

193

Table 1
Landmark Observation Cases

Case Number	Pass Number	North Latitude (deg)		Region*
		At Start	At End	
1	1	50	30	USA
2	1	50	30	USA
	2	50	30	USA
3	1	50	45	USA
	2	50	30	USA
	3	50	45	USA
4	1	50	30	USA
	2	50	30	USA
	3	65	60	Alaska
	4	65	60	Alaska
5	1	50	45	USA
	2	50	30	USA
	3	50	45	USA
	4	65	60	Alaska
	and at		20	Hawaii
	5	65	60	Alaska

*USA denotes continental USA.

attitude history that deviates from nominal by the amount anticipated in EOS. Deviations in attitude due to the various disturbing torques can be accurately indicated by the spacecraft gyros. A central force field was used for the gravity model. It was felt that the inclusion of J_2 and the higher gravitational harmo⁻⁝ ⁻vould add undue complexity to the problem without shedding any additional light on the merits of using star and landmark measurements. With the possible exception of J_2, the inclusion of the ʰⁱ harmonics does not produce a significant change in the geometry of the basⁱ⁻ ⁻ ⁻ the period of

interest (a few orbits). Consequently, if the higher harmonics were included in the simulation and were accurately accounted for in the propagation of ephemeris data (that is, no harmonic uncertainties), it is felt that the performance would be somewhat the same. With regard to the existence of uncertainties in these harmonics, it is felt that this is a problem which all techniques must face.

The nominal landmark measurement error adopted for this study was 15 meters (1σ) in downrange and crosstrack. This value does not represent the most recent estimate of what is anticipated for the proposed EOS; it merely represents the anticipated uncertainty in establishing the location of a ground control point (landmark) on the earth by other means (for example, surveying). In a more realistic situation, we would also include the error in determining the scan beam angle at the time of observation and also the errors associated with image resolution and the method used to identify landmarks in the imagery. Since most of these other sources of error had not been firmly established for EOS at the beginning of this study, they were not considered when adopting the present nominal value. This was felt to be an acceptable approach, since the plan was to generate sufficient sensitivity data to show the effect of using different values of the important error sources and parameters.

The nominal values used for the initial state uncertainties are as follows:

- Attitude (pitch, roll, yaw) — 60 arc-s (each)

- Gyro bias drift — 0.03°/hr (each)

- Ephemeris position
    a. Altitude — 20 m
    b. Downrange — 50 m
    c. Crosstrack — 20 m

- Ephemeris velocity
    a. Altitude — 0.05 m/s
    b. Downrange — 0.02 m/s
    c. Crosstrack — 0.02 m/s

In figures 3 and 4, the performance in estimating spacecraft position is shown for both the Kalman filter and the Fraser two-filter smoother. The results are for landmark observation case 4. This case, like all others, was initiated at the ascending node of the orbit and completed one pass over the north polar region before making the first pass over the United States. It is seen that the Kalman filter does an effective job in reducing the position uncertainties after two passes over the continental United States, and with only two landmark updates per pass. The significant improvement in filter performance after two passes is primarily due to the large reduction in the velocity uncertainties on the second pass. Both
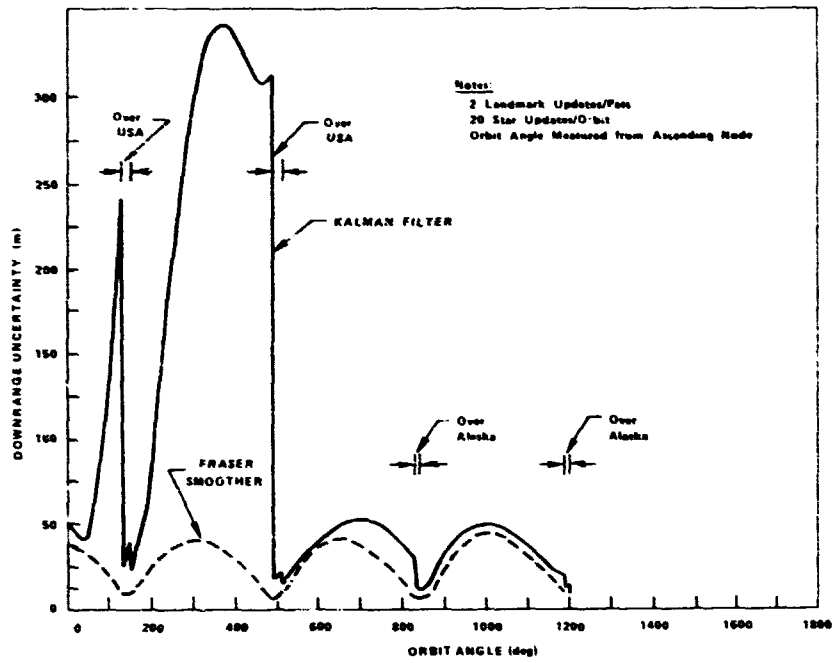
Figure 3. Kalman filter and Fraser smoother downrange estimation uncertainties for landmark observation case 4.
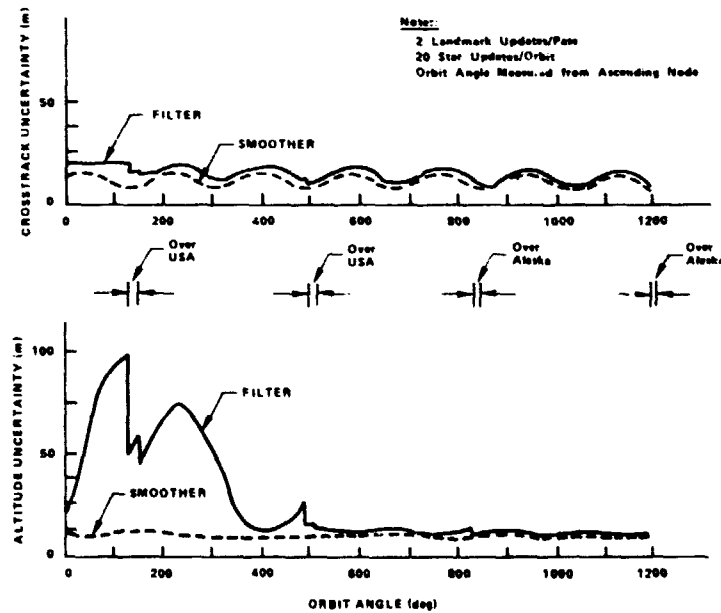

Figure 4. Kalman filter and Fraser smoother estimation uncertainties for crosstrack and altitude for landmark observation case 4.

figures 3 and 4 show that the smoother does a much better job than the filter for those portions of the orbit away from the United States. It should be noted that each smoother curve exhibits somewhat the same minimum during each pass over a landmark update region, while those for the filter are reduced from pass to pass. It is also noted that the filter performance eventually approaches that of the smoother, and it is for this reason that the filter was used in place of the more complicated smoother to generate most of the performance results of this study.

In table 2, the performance in estimating all 12 state parameters is shown for both the filter and the smoother. The filter data represents the uncertainties at the end of the last pass, while that for the smoother is for a time at the end of the first or second pass. Note that the attitude performance is very good. This is primarily due to star updates. The reason that the yaw performance is not as good as that for pitch and roll is due to the fact that very little yaw information is obtained directly from the star tracker because the stars are close to zenith.

Table 3 illustrates the performance when either landmark or star updates are not used. The first set of data is a repeat of the nominal performance of table 2 (using star and landmark updates) and is shown here for purposes of comparison with the other two data sets. The second set of data represents the performance when only landmark updates are used. It is seen that the uncertainties in pitch and downrange position (designated "range" in the table) continue to grow as one goes from landmark observation case 1 to case 5. This clearly indicates a lack of observability in this approach. It is also interesting to note that the downrange uncertainty in meters is numerically about five times larger than the pitch uncertainty in arc-seconds. Since 1 arc-s subtends about 5 m at a distance of 1000 km, the results indicate that the filter, after overcoming the initial state uncertainties, ends up applying the same equivalent update to both pitch and downrange position. The landmark measurements provide very little information to distinguish between the two state parameters. Consequently, the existing uncertainties in gyro bias drift and spacecraft velocity cause the pitch and downrange position uncertainties to grow with time. It should be noted that the same numerical relationship (5 to 1) occurs between roll and crosstrack; however, the uncertainties in these parameters do not grow with time since they are bounded by nature. On the basis of the pitch and downrange performance, it would therefore seem that there is no useful purpose to be gained in using only landmarks. However, it has been found that very strong negative correlations do occur between the errors in pitch and downrange position and also between the errors in roll and crosstrack position. These correlations are such as to greatly nullify the effects of these errors on a mapping process that makes use of attitude and ephemeris data updated with only landmark measurements.

The third set of data in table 3 shows the performance when only star updates are used. These data were generated as a matter of interest, since star measurements can only be used to update attitude and gyro bias drift. It is seen that the attitude performance is almost as good as that of the first set. The uncertainties shown for the spacecraft position components represent the natural growth of these quantities, and it is seen that the downrange position uncertainty grows more rapidly than that in the second data set.

Table 2
Kalman Filter and Fraser Smoother Estimation Uncertainties
for Different Landmark Observation Cases

Landmark Observation Case	Filter (F) or Smoother (S)	State Estimation Uncertainties (1σ)											
		Attitude (arc-s)			Gyro Bias Drift $(10^{-}{}^\circ/hr)$			Position (m)			Velocity (m/s)		
		Pitch	Roll	Yaw	X	Y	Z	Alt.	Range	Track	Alt.	Range	Track
Initial State Uncertainties (All Runs):		60	60	60	30	30	30	20	50	20	0.05	0.02	0.02
1	F	3.1	3.1	20	20	2.1	4.0	41	21	14	0.05	0.03	0.02
	S	2.5	2.3	20	20	2.1	4.0	30	18	14	0.04	0.02	0.02
2	F	1.9	1.6	14	14	0.4	1.0	14	15	10	0.02	0.01	0.02
	S	1.2	1.5	14	14	0.4	1.0	14	13	10	0.01	0.01	0.02
3	F	1.5	1.4	12	12	0.2	0.7	14	12	8	0.02	0.01	0.02
	S	0.8	1.3	12	12	0.2	0.7	14	8	8	0.01	0.01	0.02
4	F	1.3	1.3	9.8	9.8	0.1	0.6	12	11	7	0.02	0.01	0.02
	S	0.8	1.1	9.7	9.8	0.1	0.6	12	7	7	0.01	0.01	0.02
5	F	1.2	1.3	8.7	8.7	0.1	0.5	9	10	7	0.01	0.01	0.01
	S	0.8	1.1	8.7	8.7	0.1	0.5	9	7	6	0.01	0.01	0.01

Note: Smoothed data are for the time at the end of the second pass over the United States except for cases 1 and 2 where data are for the time at the end of the first pass. Filter data are for the time at the end of the last pass.

Table 3
Kalman Filter Performance for Cases With and Without Landmark or Star Updates

Landmark Observation Case	STATE ESTIMATION UNCERTAINTIES (1σ)*					
	Attitude (arc-s)			Position (m)		
	Pitch	Roll	Yaw	Alt.	Range	Track
Initial Uncertainties Are:	60	60	60	20	50	20
Nominal Performance with 2 Landmark Updates per Pass and 20 Star Updates per Orbit						
1	3	3	20	41	21	14
2	2	2	14	14	15	10
3	2	1	12	14	12	8
4	1	1	10	12	11	7
5	1	1	9	9	10	7
Performance with 2 Landmark Updates per Pass and No Star Updates						
1	44	5	32	66	213	20
2	90	5	27	54	441	20
3	161	4	22	50	782	20
4	229	4	19	38	1111	20
5	277	4	17	29	1342	20
Performance with No Landmark Updates and 20 Star Updates per Orbit						
1	3	4	24	101	291	20
2	2	2	15	101	747	20
3	2	2	12	101	1226	20
4	1	1	11	99	1712	20
5	1	1	10	99	2243	20

*Gyro bias drift and spacecraft velocity uncertainties are not shown.

Table 4 shows the sensitivity of performance to variation in the number of landmark updates per pass and the number of star updates per orbit for landmark observation case 2. It is seen that fairly good performance is obtained even with one landmark update per pass and that there is no significant improvement when going from two (nominal) to five landmark updates per pass. It is also seen in the second set of data of table 4 that some variation can be allowed in the number of star updates per orbit without seriously affecting the results.

Table 5 gives the sensitivity of performance to variation in the star and landmark measurement errors for landmark observation case 2. These data give some indication of the measurement accuracies needed in order to obtain a desired level of performance. More recent results (not shown) have been generated to show the effect of larger variations in these measurement errors.

Table 4
Sensitivity to Number of Landmark Updates Per Pass and Number of Star Updates
Per Orbit for Landmark Observation Case 2

Updates Per Pass or Orbit	State Estimation Uncertainties (1σ)*					
	Attitude (arc-s)			Position (m)		
	Pitch	Roll	Yaw	Alt.	Range	Track
Initial Uncertainties Are:	60	60	60	20	50	20
Landmarks**						
1	1.9	1.6	15	16	18	11
2 (Nom.)	1.9	1.6	14	14	15	10
3	1.9	1.6	14	13	13	9
5	1.9	1.6	12	13	12	9
Stars**						
5	3.3	2.5	19	13.4	21	13
10	2.5	2.1	18	13.4	17	11
15	2.1	1.8	16	13.4	16	10
20 (Nom.)	1.9	1.6	14	13.4	15	10
25	1.7	1.5	12	13.4	14	10

*Gyro bias drift and spacecraft velocity uncertainties are not shown.

**Other type measurement (star or landmark) was nominal.

Table 5
Sensitivity to Star and Landmark Measurement Error for Landmark Observation Case 2

Measurement Error (1σ) (Per Axis)	State Estimation Uncertainties (1σ)*					
	Attitude (arc-s)			Position (m)		
	Pitch	Roll	Yaw	Alt.	Range	Track
Initial Uncertainties Are:	60	60	60	20	50	.20
Star Measurement Error						
2 s	0.8	0.8	7	13.3	12	8
5 s	1.9	1.6	14	13.5	15	10
10 s	3.6	2.7	18	13.8	21	13
15 s	5.4	3.3	20	14.1	29	16
Landmark Position Error (Downrange and Crosstrack)						
7.5 m	1.9	1.6	12	10	11	8
15 m	1.9	1.6	14	14	15	10
30 m	1.9	1 7	15	16	24	13
45 m	1.9	1.7	15	16	34	16

*Gyro bias drift and spacecraft velocity uncertainties are not shown.